Spring 3-30-2024

An Injectable In Situ Forming Collagen/Alginate/CaSO4 Composite Hydrogel for Tissue Engineering Applications: Optimization, Characterization and In Vitro Assessments

samar A. salim
The British University in Egypt, samar.salim@bue.edu.eg

samar A. salim
The British University in Egypt

Arabian Journal for Science and Engineering
https://doi.org/10.1007/s13369-024-08922-w

RESEARCH ARTICLE-CHEMISTRY

An Injectable In Situ Forming Collagen/Alginate/$CaSO_4$ Composite Hydrogel for Tissue Engineering Applications: Optimization, Characterization and In Vitro Assessments

Hamsa Ashraf[1] · Samar A. Salim[2] · Shahira H. EL-Moslamy[3] · Samah A. Loutfy[2,4] · Elbadawy A. Kamoun[5,6,7]

Received: 14 September 2023 / Accepted: 29 February 2024

Abstract

In situ injectable hydrogels are effectively employed to fill irregular cavitary bone defects with initiating bone growth in targeted areas. Herein, an injectable composited hydrogel composed of collagen and alginate cross-linked *in situ* using different concentrations of calcium sulfate (0.15, 0.3 and 0.6%, wt./v) was synthesized. Recently, $CaSO_4$ is frequently supported as a bone graft material for bone regeneration, owing to its biocompatibility and osteoconductive properties. Moreover, hydroxyapatite (Hap) after salinization-step by (3-Aminopropyl) triethoxysilane (APTES) was incorporated for further enhancing the osteoconductive property of injected hydrogels. All fabricated hydrogels were characterized by SEM, FTIR and XRD analyses. While physiochemical characteristics of hydrogels were assessed through swelling index, hydrolytic degradability and thermal stability measurements. *In vitro* bio-assessments, *e.g.,* antimicrobial activity, cytotoxicity and cell adhesion tests using osteoblast-like cells (*MG-63*) were investigated. Results showed that addition of Hap offered better control of gelation time and formed uniform hydrogels, additionally improved significantly thermal stability, which leads to hindering of swelling index, prolonging hydrolytic degradability rates and significantly enhanced the antimicrobial activity of hydrogel; compared to hydrogel free-Hap. Hap-loaded Col–Alg–$CaSO_4$ hydrogel with the highest concentration of $CaSO_4$ recorded an enrichment of cell viability among all hydrogel samples. Notably, *In vitro* cell adhesion test showed that *MG-63* cells adhered adequately with all hydrogels. The results support the approach of using an injectable Hap-loaded Col/Alg hydrogel cross-linked with $CaSO_4$ as an alter and novel technique to enhance bone tissue regeneration, host–implant integration, quick/simple technique and easier for clinical handling.

Keywords Collagen/alginate · $CaSO_4$ · Composite hydrogels · Hydroxyapatite · Bone regeneration

1 Introduction

Biomaterials engineering can offer a substitute solution for bone regeneration and repair [1]. A general idea about tissue engineering includes fabricating of a biomaterial scaffolds integrate with the cells, where it intacts and suitable for the signaling factors [2].

This biocompatible construct can be implanted into the body to promote tissue regeneration. The scaffold can be composed of either natural, synthetic, or both polymers and can be fabricated into a hydrogel, fibrous or 3D structure [3]. It has been widely studied in the hope of reaching the optimal

✉ Elbadawy A. Kamoun
ekamoun@kfu.edu.sa

1 Regenerative Medicine Laboratory, Department of Basic Research, Children's Cancer Hospital 57357, Cairo, Egypt

2 Nanotechnology Research Center (NTRC), The British University in Egypt (BUE), Cairo 11837, Egypt

3 Bioprocess Development Department (BID), Genetic Engineering and Biotechnology Research Institute (GEBRI), City of Scientific Research and Technological Applications (SRTA-City), New Borg El-Arab City, Alexandria 21934, Egypt

4 Virology and Immunology Unit, Cancer Biology Department, National Cancer Institute, Cairo University, Cairo, Egypt

5 KFU, Saudi Arabia

6 Department of Chemistry, Collage of Science, King Faisal University, 31982 Al-Ahsa, Saudi Arabia

7 Polymeric Materials Research Dep., Advanced Technology and New Materials Research Institute (ATNMRI), City of Scientific Research and Technological Applications (SRTA-City), Alexandria 21934, Egypt

Published online: 30 March 2024

construct. Many tissue engineering designs for orthopedic applications are using the approach of injectable hydrogel in situ cross-linking forming systems. In comparison with other forms of scaffolds, injectable hydrogel has a unique property that it can reach defects or areas of the body using a minimally invasive needle implantation procedure and has the ability to occupy the space of any type of defect geometry and prevent the entrance of the fibrotic tissue [4]. In addition, the injectable hydrogel can be used as a carrier for stem cells, growth factors and therapeutic agents such as drugs [3]. Biocompatibility is the most important requirement of optimal injectable hydrogel to perform its application without inducing immunologic response or avoiding being cytotoxic for the transparent cells, tissues or organs. Injectable hydrogel should also be biodegradable, have mechanical properties close to the bone, and have adhesive and cohesive properties to intact inside the defect [4, 5]. In terms of clinical handling, it should be easily prepared during the surgical time and has rapid gelation time. Furthermore, from an industrial point of view, it should also be cost-effective and be stable during storage [6]. Fabricating a hydrogel with these optimal characteristics considers being a promising candidate for the tissue engineering field.

Cross-linking techniques of materials in scaffolds have been widely investigated [7, 8]. Sol–gel polymerization, including photo-polymerization, thermal, enzymatic, chemical cross-linking systems and different additional mechanisms, are applied to allow the creation of cross-linking between materials [3, 6, 7]. Radical chain polymerization is meant that photo-initiators or redox initiators are involved to generate free radicals to initiate the cross-linking process [7]. Similarly, most thermo-gelation and chemical cross-linking systems involve the modification of polymeric chains with non-degradable backbones, such as N-isopropylacrylamide (pNiPAAm), glutaraldehyde are used in thermo-gelation and chemical gelation techniques, respectively [6, 9–11]. However, these types of modification or initiators introduce side groups or cross-linker. They have potential cytotoxic agents and cause additional adverse immune responses. These types of cross-linking systems are less biocompatible for purposes of injectable hydrogel and causes toxicity toward the cells [6, 8]. Therefore, using injectable systems without involving toxic photo-initiators or polymeric modifications for example, ionic cross-linked systems has more applicability as biocompatible injectable hydrogel. Ionic cross-linked injectable hydrogel systems including cheap and cost-effective natural polymers such as alginate are extensively studied and have been used in various biomedical purposes such as wound dressing, cell therapies and bone engineering scaffolds [12].

Natural polysaccharide such as alginate can be extracted from natural sources, such as *Macrocytis pyrifera* (kelp) as a type of brown algae and has a linear copolymer structure, which has chemical compound consists of repeated blocks of (1–4) linked α-*L*-guluronate (G blocks) and β-*D*-mannuronate (M blocks) with various proportions and sequential arrangements of MG blocks [3]. It was recorded by Grant et al. that the G blocks of alginates form an egg-box structure when interacting with calcium, barium and strontium [13]. The divalent cations cause the two deprotonated carboxylate groups of one G block to be bonded with two hydroxyl groups of another [12]. Hence, sol–gel transition of alginate occurs due to the lateral egg-box multimers cross-linked and the concentration of divalent cations highly influences the rate and kinetics of cross-linking [14]. The disadvantage of applying alginate as a hydrogel In vitro, it limits cells to attach, because of its highly hydrophilic and negatively charged properties [15], which hinders its application in bone regeneration. Therefore, fabrication of hydrogel, that resembles the natural bone, increases its osteogenic potential and bone regeneration. Many studies studied to support the alginate properties by another copolymers such as chitosan and collagen [12, 16].

Collagen is the most ample protein in mammals as well as is the most frequently utilized in tissue engineering in different forms like sponges, fibrous membranes or hydrogel matrices; also, its main source is bovine tissue [17]. Collagen hydrogel is suitable for bone regeneration because of its porous structure, enhancement of cell attachment, hydrophilicity, biodegradability and permeability [18, 19].

Calcium sulfate ($CaSO_4$) was used as a cross-linker/gelling agent for alginate to form sol–gel polymerization [3]. $CaSO_4$ is one of the frequently utilized materials for bone tissue regeneration [20]. Most of the animal and clinical studies showed the accomplishment of using $CaSO_4$ as bone graft material for more than one hundred years due to its biocompatibility without inducing the inflammatory responses [20, 21]. The advantages of $CaSO_4$ were found as it possesses osteoconductive and biodegradable properties in comparison with other cement materials [22]. However, the low mechanical property of $CaSO_4$ is one of its drawbacks, mechanical properties such as bending strength and fracture toughness [23]. Therefore, the greatest used approach to increase the mechanical property of scaffold is by adding Hap [24].

Hydroxyapatite or calcium phosphate $Ca_{10}(PO4)_6(OH)_2$ nanoparticle is a natural substance present in the extracellular matrix composition of teeth, bone and tendons, which is the main factor for their high mechanical property [25]. The key advantage of Hap is its osteo-inductive properties, which allow integration of host tissue with the biomaterial forming an adequate interface without the formation of an inert surface. This offers a faster and better tissue integration and hence, higher capability of tissue regeneration [24]. However, bone growth usually occurs on the surface of Hap, due to its partial bioactivity. Hence, functionalization of Hap with

free amino acids has shown a promising way to increase its bioactivity [24, 26]. One of the known research-based techniques to bind free amino acids is by adding 3-aminopropyl triethoxysilane (APTES) to Hap particles [26].

This work aims to develop *In situ* injectable composite hydrogel without inducing toxic cross-linkers to heal bone fractures and cavity defects. Hydrogels explored optimal properties e.g. cost-effectiveness, biocompatible, biodegradable, antimicrobial, in addiiton hydrogels have suitable gelation rate and quick time preparation for easier clinical handling. We investigated the addition of different concentrations of $CaSO_4$ as an alternative cross-linker to Hap-loaded and unloaded collagen/alginate composite hydrogel to obtain injectable hydrogel with optimal physical properties. Appropriate biological characteristics including biocompatibility and cell attachment were assessed and discussed to prove its biological prospective as injectable regenerative biomaterial.

2 Materials and Methods

2.1 Materials

Calcium sulfate anhydrous ($CaSO_4$) (Mwt. 136.14 g/mol) was purchased from Alpha Chemika, India. Collagen A (Mwt 300 KD) in a liquid form (1 mg/ml) and alginic acid sodium salt powder, viscosity 1%, H_2O, (Mwt. 120–190 KD), nano-hydroxyapatite (Hap) (< 200 nm particle size (BET) containing 5 wt. % silica as dopant) and 3-aminopropyl triethoxysilane (APTES) were obtained from Sigma-Aldrich Co., Steinem, Germany. The tested human pathogens (*Pseudomonas aeruginosa*, *Escherichia coli*, *Bacillus cereus*, *Staphylococcus aureus*, *Candida albicans* and *Candida krusei)* were received from Bioprocess Development Dep, GEBRI, SRTA-City, Alexandria, Egypt.

2.2 Salinization Reaction of Hydroxyapatite (Hap) with APTES

Russo et al. functionalized Hap nanoparticles by using APTES [26] as surface modifier agent. Typically, 1.1 g of Hap is dispersed well in 12.5 ml of deionized water (DW) under continuous stirring for 2h at 60 °C, resulting in the Hap hydrolysis. Then, 2 ml of APTES is added in a dropwise manner 0.07 ml/min (~ 1.0 ml every 15 min) to get milky suspended solution of Hap. The suspended Hap solution is incubated at 60°C for overnight. The suspension is centrifuged at 3000 rpm for 30 min, and then, APTES-Hap is washed with DW several times to get rid any unbounded APTES. After the washing steps at 60 °C, APTES-Hap is dried for 6 h, and then, it is grounded by using a porcelain mortar and the resultant APTES-Hap is stored in a dry and cold environment to be used for further steps.

Table 1 Compositions of Col–Alg–$CaSO_4$ hydrogels and physical observation of formed composite hydrogels

Col–Alg–$CaSO_4$ composite hydrogels		
Col: Alg, (w/v, %)	$CaSO_4$, (w/v, %)	Physical observation
0.01: 0.8	0	No hydrogel formed
	0.07	No hydrogel formed
	0.15	Homogenous hydrogel formed
	0.30	Homogenous hydrogel formed
	0.60	Preparatory and sudden hydrogel formed

Table 2 Additional effect of $CaSO_4$ concentrations on the formation of Col–Alg-Hap-$CaSO_4$ composite hydrogels

Col–Alg-Hap-$CaSO_4$ composite hydrogel		
Col: Alg: Hap, (w/v, %)	$CaSO_4$ (w/v, %)	Physical observation
0.01: 0.8: 1.6	0	No hydrogel formed
	0.15	No hydrogel formed
	0.30	Homogenous hydrogel formed
	0.60	Homogenous hydrogel formed

2.3 Preparation of Injectable Col–Alg–$CaSO_4$ Composite Hydrogel

Col–Alg–$CaSO_4$ hydrogels are fabricated by utilizing the stock solution of 0.1% collagen (wt./v), and 2% alginate (wt./v) in DW and $CaSO_4$ is prepared with adding different concentrations of (0, 0.07, 0.15, 0.3, 0.6%, wt./v) in DW under ultra-sonication to obtain the full dispersion solutions as shown in Table 1. The gelation time is monitored by the test tube-tilting method [3]. Every 30 s, the falcon tube is tilted 90° after initial mixing time and when the composite solution does not move any longer, this is assigned as the gelation point [1]. It is noticed that there is no difference or a correlation in the gelation time and the period time of alginate/collagen which were mixed before addition of $CaSO_4$, where the average period was around one hour.

The bioactive salinized-Hap NPs are similarly incorporated as a suspended solution in DW into the hydrogel with a fixed concentration of 1.6% (wt./v) and different concentrations of $CaSO_4$ as shown in Table 2. Gel yield is also determined to obtain the percentage of formed hydrogel from

each solution through calculating the final weight of hydrogel formed (Wf) *vs.* the initial weight (Wi) of the solution before hydrogel formed [27], as given formula in Eq. (1).

$$\text{Gelyield(hydrogel\%)} = \left(\frac{Wf}{wi}\right)x100 \quad (1)$$

2.4 Characterizations of Injectable Col–Alg–$CaSO_4$ Composite Hydrogel

All prepared composite hydrogels are subjected to a series of characterization tests: *FTIR*: The functional groups and chemical structure of alginate, collagen, modified Hap and all fabricated hydrogels are analyzed by FTIR (IR, 8400s Shimadzu, Japan) with IR fingerprints recorded 4000–400 cm^{-1}. *XRD*: The composition of inorganic components present in the composite hydrogels is determined by using X-Ray diffraction (XRD, Malvern Panalytical Empyrean 3). Scans are collected with a scan rate of 0.21 per minute with Cu Kα X-ray (λ = 1.54056 Å, 40 kV, 250 mA). *SEM*: The morphologies of different composite hydrogel surfaces are analyzed by (SEM, Joel GSM-6610LV, Japan). All samples are investigated without coating using low vacuum during investigation and low voltage at 5 kV to avoid samples-shrinkage and deformed. *TGA*: Thermal stability of the composite hydrogel is conducted using a TG analyzer ((TGA50, Shimadzu, Japan) to determine the weight loss %. Dried hydrogels are investigated under N_2 gas at heating rate of 10 °C/min and temperature ranged 25–550 °C.

2.5 Physiochemical Properties of Injectable Col–Alg–$CaSO_4$ Composite Hydrogel

2.5.1 Swelling Index (SI)

Each hydrogel is weighed (W1) and immersed into a beaker with 10 ml of PBS. The samples' weight is recorded at interval times by removing from DW and wiping off the extra water [24]. The swollen hydrogels are re-weighed (W2) versus the weight change of each hydrogel, as given in *Eq.* (2).

$$SI = (W2 - W1)/W1 \quad (2)$$

2.5.2 Hydrolytic Degradation Index (DI)

To investigate the relative amount of weight loss (%) from different composite hydrogels, each hydrogel is designed in a fixed format and weighed. Each part is put in 10 mL of buffer and retained in an incubator at room temperature for interval times. Subsequently, each part is wiped off extra buffer and re-weighed, after that compared with the original weight. The degraded hydrogels are re-weighed (W2) and the loss of each hydrogel is determined depending on the weight loss for each hydrogel as given in *Eq.* (3) [24].

$$DI = (W1 - W2)/W1 \quad (3)$$

2.6 In Vitro Evaluation of Composite Hydrogels

2.6.1 Antimicrobial Activity

Antimicrobial bioassays *In vitro*: well diffusion method and the micro-broth-dilution assay are used [28], to evaluate the antimicrobial potency of various composites made of Hap, collagen, alginate and $CaSO_4$.

Well-Diffusion Method The antimicrobial activities of all of those formulations are evaluated using the agar well diffusion method, as previously described [29]. The pathogen cultures are recharged by inoculating them in a rich LB Broth medium produced by dissolving (10 g of tryptone, 10g of NaCl and 5 g of yeast extract in 1L of DW). These cultures are then incubated for 24h at 37 °C and 200 rpm. Following that, an aliquot of these pre-cultures (2×10^5 CFU/ml) is prepared with sterile saline (0.8% NaCl). A sterile *Petri* dish was filled with 1ml of these pre-cultures and then gently mixed with 20 ml of the molten LB medium. After the agar plates had solidified, a sterilized cork-borer was used to drill wells into the plates (6 mm). The wells are then filled with 100 µl of each formula. The plates are refrigerated for 30 min to permit the formula to completely diffuse into the agar. These plates are further incubated at 37 °C for 24h. The inhibition zone is determined to estimate the inhibitory impact after the incubation period.

Broth Micro-Dilution Method 0.5 McFarland turbidity standards are used, where an overnight culture pathogen was produced by LB broth [4]. Except the control samples, all these cultures are treated with distinct formulations. These tubes are then cultivated for one night at 200 rpm and 37 °C. On a timely manner, aliquots of each culture and its controls are sampled to estimate the quantitative evaluation of the absorbance of turbidity at 600 nm. All attempts that are carried out triplicated to reduce errors and get the mean ± SD.

2.6.2 Cytotoxicity Test

All hydrogels with different composition can be represented as follows: Col–Alg–$CaSO_4$ (0.15%) Col–Alg–$CaSO_4$ (0.30%), Col–Alg–$CaSO_4$ (0.60%), Col–Alg–$CaSO_4$ (0.30%)-Hap and Col–Alg–$CaSO_4$ (0.60%)-Hap, which are tested for their biocompatibility on human osteoblast cell

line, e.g., (*MG-63* cells) using MTT assay as earlier reported by Salim et al. [24]. *MG-63* cell line is sub-cultured and kept in DMEM media containing (FBS (10%)), and antibiotics (100 IU/mL penicillin/streptomycin was obtained from Lonza, Belgium) at 37 °C under a humidity of 5% CO_2. Lastly, cells were passaged usually by trypsinization (*i.e.,* trypsin/versine, and 0.05%, Lonza). The hydrogels were soaked in a culture medium at an extraction ratio of 1 mg/ml and incubated at 37 °C under a humidified atmosphere with 5% CO_2, for 24h, as was previously demonstrated by Thi-Hiep et al. [30]. MTT test based on dye reduction by mitochondrial dehydrogenases of live cells into insoluble formazan crystals is carried out typically. Briefly, cell monolayers are incubated with hydrogels for 48h before exposure to MTT solution in PBS (5 mg /mL) and incubated for 4h. DMSO (100 mL per well) was added under shaking for 10 min to remove the formazan crystals. The measurement of absorbance is at 540 nm against blanks (media only) in a microplate reader. Cell survival index is determined by matching the optical density (OD) of DMSO control wells with ODs of the samples and shown as viability % to the control. The dose–response experiment is performed on samples producing $\geq$ 50% loss of cell viability after cell treatment with two-fold serial dilutions (200, 100, 50, 25, 12.5 and 6.25 μg/mL) of samples. All tests are done in triplicates and the relative cell viability (%), compared to control wells containing *MG-63* without hydrogels, was determined via the following formula: (A) test/(B) control $\times$ 100%.

2.6.3 Cell Adhesion Test

Cell adhesion test for *MG-63* on composite hydrogel is done as previously described elsewhere [31]. Briefly, plates are coated with composite hydrogels with different compositions labeled as HA1; Col–Alg–$CaSO_4$ (0.15%), HA2; Col–Alg–$CaSO_4$ (0.30%), HA3; Col–Alg–$CaSO_4$ (0.60%) HA4; Col-Alg-Hap- $CaSO_4$ (0.30%) and HA5; Col-Alg-Hap-$CaSO_4$ (0.60%). Five hundred μl of *MG-63* suspension at density of (1×10^5) cells/ml is seeded into 24-well hydrogel-coated plate. *MG-63* cells are incubated at 37°C under 5% CO_2 for 3h. After washing the cells with PBS twice, the adhered cells are fixed using 15% formalin in PBS for 15 min. After fixation, cells are washed twice with PBS and stained for 15 min with 0.05 g/ml crystal violet at 37°C. The plates are shaken gently at room temperature for 10 min, where the cells number in each well are counted in three microscopic fields (magnification $\times$ 10) and images are taken using ZEISS *Axio Observer 5*.

2.7 Statistical Analysis

All data are collected from at least three distinct experiments and are reported as means and standard deviations (M $\pm$ SD). The results of each group are statistically compared by one-way analysis of variance (*ANOVA*) software and *Tukey* multiple/post hoc comparisons test (P value < 0.05) via *Minitab 18-Graph pad* software.

3 Results and Discussion

3.1 Gelation Time and Gel Yield (%) of Formed Col–Alg–$CaSO_4$ Composite Hydrogels

The average gelation time of Col–Alg–$CaSO_4$ composite hydrogel with different $CaSO_4$ concentrations (0, 0.15, 0.30 and 0.60%, wt./v) is shown in Fig. 1. Basically no hydrogel formed with hydrogel containing $CaSO_4$ concentration less than 0.15 wt./v % is noticed, and as $CaSO_4$ increases from 0.15 to 0.60%, the gelation time decreases significantly from 40 to 15 s. However, increasing the gelation time causes more inhomogeneous hydrogel, due to rapid alginate gelation, which caused difficulty of the calcium ions to diffuse through the immediate gelled formed parts, leading to unreacted alginate. The alteration of the gelation time with $CaSO_4$ concentration is recorded, due to the increase in the calcium concentration which allow more calcium ions to cross-link the G blocks of alginate through forming the *egg-box* structure in a shorter time [3].

Moreover, addition of salinized Hap to the hydrogel prolongs the gelation time as function of $CaSO_4$ concentrations in hydrogels, comparing to the hydrogel without adding Hap. Results show that no hydrogel was formed in case Col-Alg-Hap-$CaSO_4$ with 0.15 wt./v, % of $CaSO_4$. It was explained that the main composition of Hap is calcium phosphate which is an extra source of calcium to react with alginate and forming hydrogel. However, calcium in Hap has higher stability and lower solubility than the free $CaSO_4$. It was noticed that the stability of calcium ion in $CaSO_4$ compound is lower than that in calcium phosphate [3], causing quicker gelation time. It was previously tested that the usage of a calcium source with lower solubility and high stability leads to a gradual increase in gelation rate, avoiding an immediate gelation [3]. Interestingly, addition of Hap reduced the gelation time from 30 to 10 s, when $CaSO_4$ is increased from 0.30 to 0.60 wt./v, % (Fig. 1). Also, the gel yield/gel fraction was measured to get the most completely gelled solution and to exclude any excess of unbounded material. As shown in Table 3, the gel yield of the different fabricated hydrogel composition was more than 66%. HA1; Col–Alg–$CaSO_4$ (0.15%), HA2; Col–Alg–$CaSO_4$ (0.30%), HA3; Col–Alg–$CaSO_4$ (0.60%),

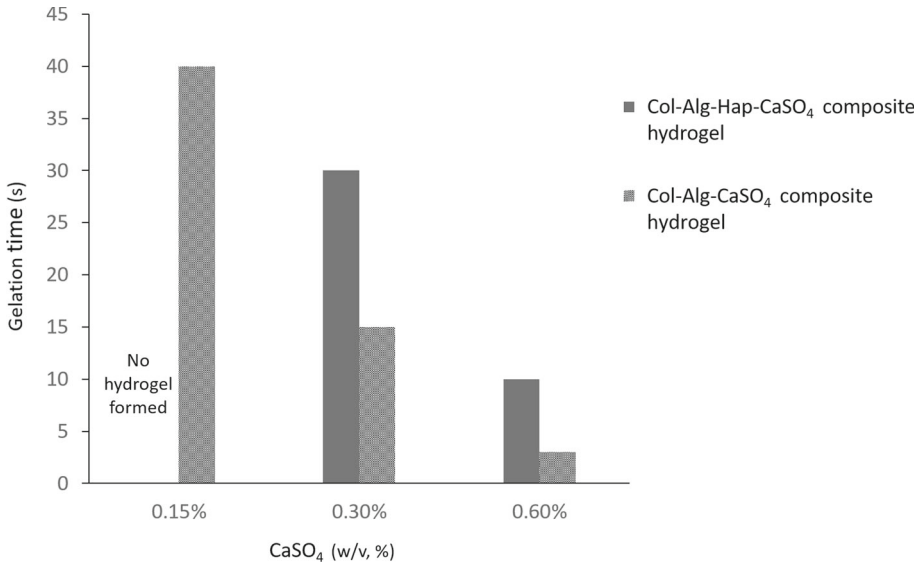

Fig. 1 Effect of different $CaSO_4$ concentrations in formed Col–Alg–$CaSO_4$ and Col-Alg-Hap-$CaSO_4$ on the average gelation time of formed composite hydrogels

Table 3 Additional effect of $CaSO_4$ concentrations on the gel yield % of formed Col-Alg-Hap-$CaSO_4$ composite hydrogels

Composite hydrogels	Col: Alg w/v, %)	Hap (w/v, %)	$CaSO_4$ (w/v, %)	Gel yield (%)
HA1; Col–Alg–$CaSO_4$ (0.15%)	0.01: 0.8	0	0.15	94
HA2; Col–Alg–$CaSO_4$ (0.30%)		0	0.30	96
HA3; Col–Alg–$CaSO_4$ (0.60%)		0	0.60	96
HA4; Col-Alg-Hap-$CaSO_4$ (0.30%)		1.6	0.30	86
HA5; Col-Alg-Hap-$CaSO_4$ (0.60%)		1.6	0.60	66

HA4; Col-Alg-Hap-$CaSO_4$ (0.30%) and HA5; Col-Alg-Hap-$CaSO_4$ (0.60%).

3.2 FTIR Analysis of Col–Alg–$CaSO_4$ Composite Hydrogels

Figure 2 shows the spectra of different Col–Alg–$CaSO_4$ composite hydrogels. As realized, the alginate spectrum shows different characteristics bands, such as COO-modes, found at ν 1428 and 1628 cm^{-1}, also stretching C–O modes happened at ν 1080 cm^{-1}, as well as OH vibration peak at ν 3465 cm^{-1}. Furthermore, blended OH group of carboxyl occurred at ν 889 cm^{-1}. Addition of collagen leads to a shift of COOH absorption bands to a higher wavenumber. After addition of collagen and alginate together, it was shown that a disappearance of NH group at ν 3423 cm^{-1} linked to collagen spectrum and disappearance of distinct band of OH group of alginate spectrum, which is found as an obvious indicator for successful entanglement between OH group of alginate and NH group of collagen. By comparing spectra of Col–Alg-Hap-$CaSO_4$ hydrogel and either alginate or collagen only, a distinct shift to a slightly lower wavenumber occurred. It was elsewhere reported that the proposed shift was an indication of the bond between organic and inorganic phases in the hydrogel, which supports that NH of salinized Hap was bonded with carboxyl and OH group of collagen and alginate [32].

The salinization reaction of Hap is confirmed by FTIR analysis, as shown in Fig. 3. The vibrational peak of PO_4^{-3} groups of unmodified Hap is recorded at ν 1200–965 cm^{-1} and ν 600–500 cm^{-1}. APTES- Hap nanoparticles is indicated by the appearance of distinct intensive band in the region of ν 1100–1200 cm^{-1} which shows the presence of asymmetric stretching of siloxane group Si–O–Si. Additionally, the verification of salinization reaction of Hap is confirmed by the presence of ν 1390 cm^{-1}, which indicates to NH_2 formation [26].

3.3 XRD Analysis of Modified Hap-APTES

XRD is used to elucidate the active components of the modified Hap with APTES. X-ray diffraction patterns of unmodified Hap, APTES and modified APTES are shown in Fig. 4. The modified Hap shows typical diffraction patterns of unmodified Hap nanoparticles, which are in agreement

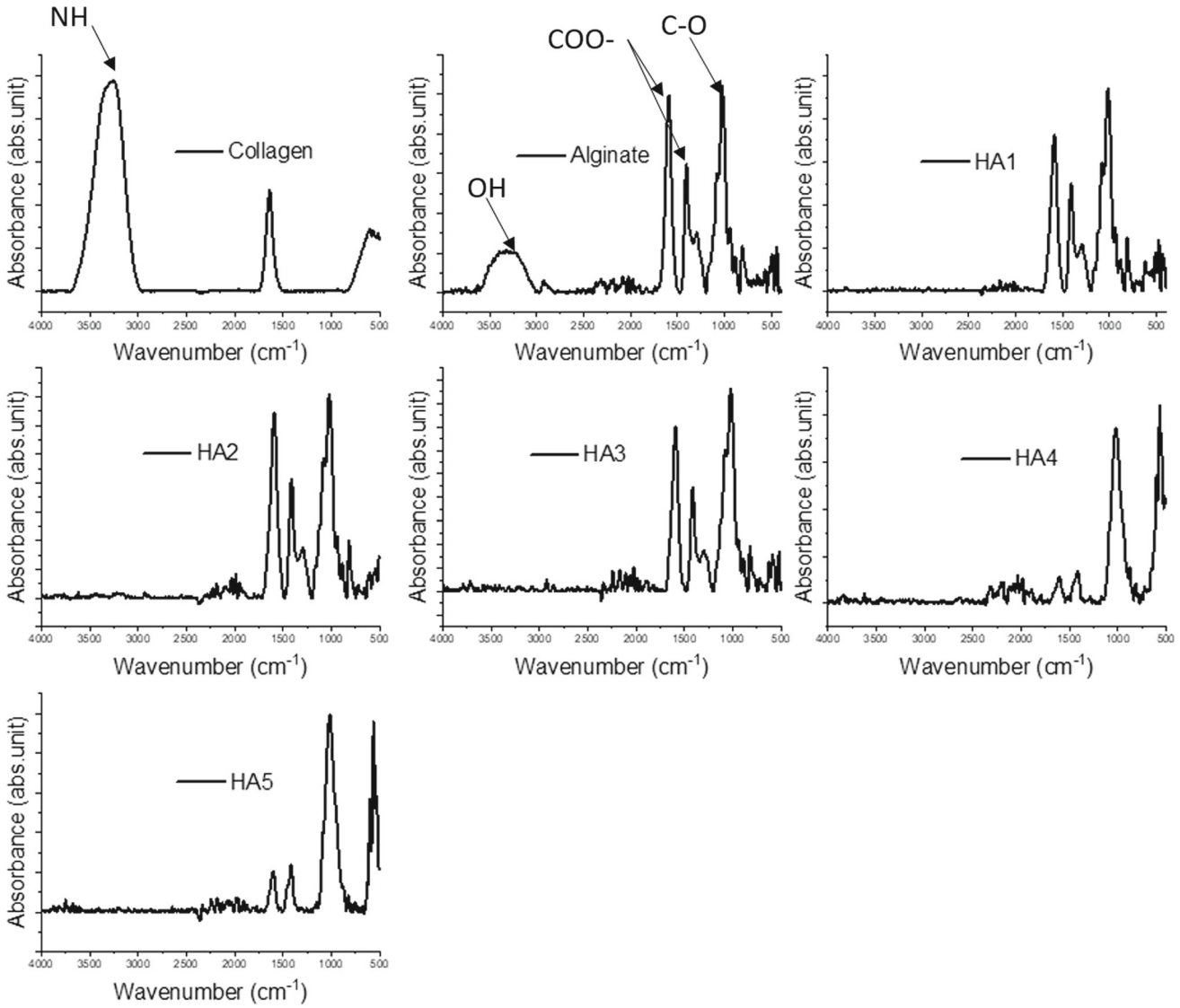

Fig. 2 FTIR spectra of collagen, alginate and selected Col–Alg–$CaSO_4$ composite hydrogel

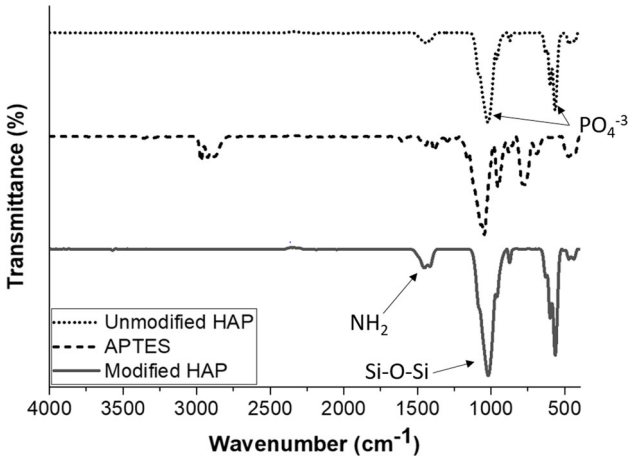

Fig. 3 FTIR spectra of unmodified hydroxyapatite (Hap), Hap-APTES and APTES

with inorganic crystal structure database standards (ICSD) reference (26,204) and previous reported results [33]. Sharp characteristic peaks of nano-Hap are shown at 2θ around 25°, 29°, 32°, 46° and 49°. In the addition of APTES to functionalize Hap, all detected diffraction peaks of Hap-APTES overlapped with the diffraction peaks of unmodified Hap and APTES [19, 26].

3.4 SEM Investigation of Col–Alg–$CaSO_4$ Composite Hydrogels

SEM investigation is always employed to provide insight of morphology and the surface featured structural of hydrogels. Figure 5 shows the surface morphology of various hydrogels and its porous structure. Figure 5 shows that the addition of Hap in hydrogels formulas of HA4 and HA5 exhibits

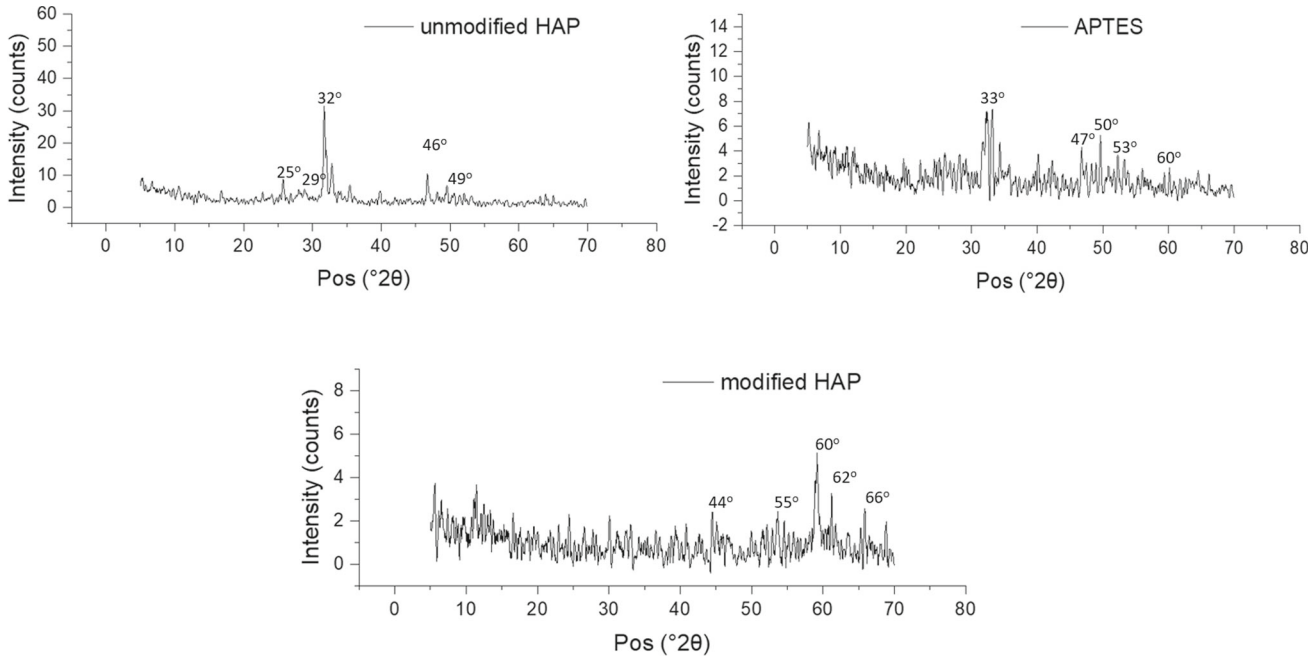

Fig. 4 XRD patterns of unmodified hydroxyapatite (Hap), Hap-APTES and APTES

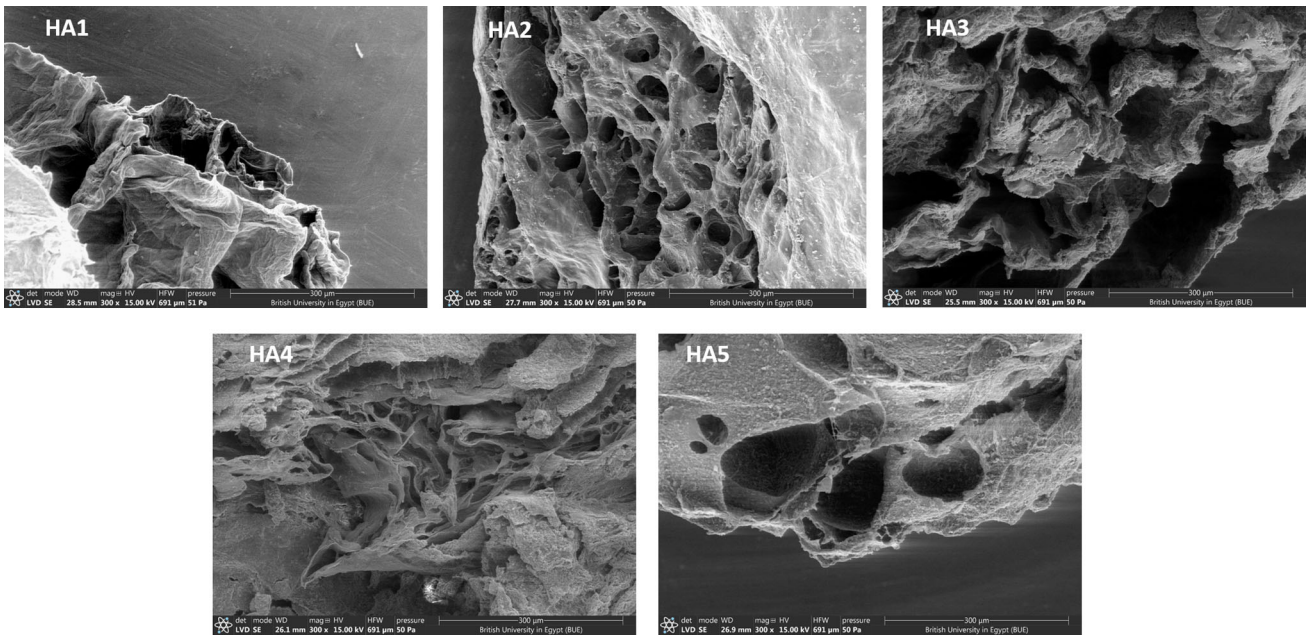

Fig. 5 SEM images of selected composite hydrogels. HA1: Col–Alg–$CaSO_4$ (0.15%), HA2: Col–Alg–$CaSO_4$ (0.30%), HA3: Col–Alg–$CaSO_4$ (0.60%), HA4: Col-Alg-Hap-$CaSO_4$ (0.30%) and HA5: Col-Alg-Hap-$CaSO_4$ (0.60%); (*original magnification X300 at 15 kV with scale 300 μm*)

a rougher and irregular surface compared to HA1, HA2 and HA3 hydrogels. Previously, incorporation of Hap particles and surface roughness improved cell attachment and enhancement of cell proliferation and osteogenic differentiation [24, 34, 35].

3.5 Physicochemical Properties of Col–Alg–$CaSO_4$ Composite Hydrogels

3.5.1 Swelling Index

Swelling study of prepared hydrogel is one of the most critical factors for adaptation of biomaterial inside the body [24]. The

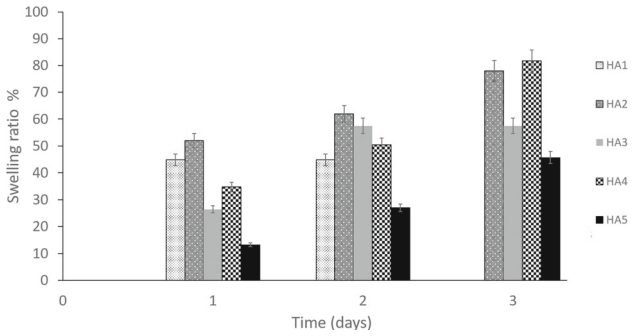

Fig. 6 Swelling index of Col–Alg–$CaSO_4$ composite hydrogels without and with hydroxyapatite

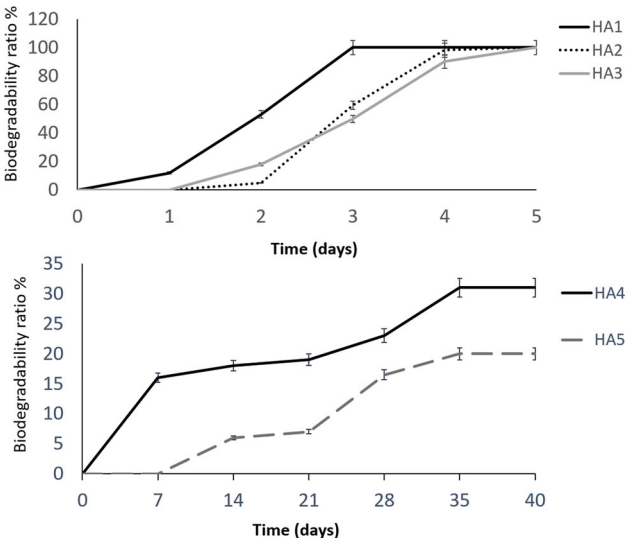

Fig. 7 Hydrolytic degradation of Col–Alg–$CaSO_4$ composite hydrogels without and with hydroxyapatite over 8 and 45 days, respectively

swell-ability degree of scaffold is an important indicator for how the material will perform under high humidity condition inside the body [36]. The formed hydrogels are hydrophilic that can soak the surrounded water at 37 °C and allow the formation of porous structure, aiding in adequate nutrition and oxygen movement inside and outside the cells as well as allowing cell signaling [24]. All selected hydrogel is able to swell in distilled water and PBS. There is a significant difference between the swelling degradability among the five hydrogel formulas, as shown in Fig. 6.

It is observed that the swelling ratio after three days of HA1 hydrogel is 45%, which is significantly lower than HA2 hydrogel of 80%. This indicated that the concentration of $CaSO_4$ as a cross-linker increases, more polymer chains are being formed, increases the surface area of the composite hydrogel and the number of hydrophilic functional groups including carboxylic, amide and alcohol groups in the polymeric network is also increased. This leads the composite to have a higher capacity of allowing the solvent, water, to penetrate the void spaces of the polymeric chain network body [36]. However, HA3 hydrogel shows an opposite behavior of the mentioned results, where it records lower swelling ratio than HA2 hydrogel and this could be due to increase the added concentration of $CaSO_4$. It is indicated before that there is basically an inverse relationship between the cross-linking degree and swelling degree of hydrogel or biomaterial [37]. The decrease in swelling ratio of HA3 could be owing to increase in the cross-linker causes more cross-linking of alginate with calcium ions of $CaSO_4$.

It is observed that Hap addition does not expressively affect the swelling rate of HA4 hydrogel (*ca.* 80%), with similar swelling rate as HA2 (79%). However, it is observed that the swelling degree of HA5 is recorded ~ 45% at day 3, and is the slowest swelling rate compared to other hydrogels. This demonstrates that the addition of Hap with increase in the concentration of $CaSO_4$ reduces the swelling degree of hydrogel. Likely, increasing the concentration of ceramic material including incorporated Hap and $CaSO_4$ into the scaffold reduced the swelling rate, owing to the interaction between Hap/$CASO_4$ NPs with the OH groups of polymers [24], which lead to swelling reduction.

3.5.2 Hydrolytic Degradation (%)

Alginate, collagen, Hap and $CaSO_4$ are generally biocompatible and have lower toxicity potential at the molecular, cellular or organ level. Therefore, they do not create unwanted toxic by-products after its degradation process [36]. The time of degradation should complement with the time of newly bone tissue ingrowth inside the defect [31]. As shown in Fig. 7, the degradation rate of hydrogel in PBS solution at 37 °C is determined by calculating the weight loss. Notably, increasing the concentration of $CaSO_4$ has an inverse relationship against degradation rate of composite hydrogels. Weight loss (%) of Col–Alg–$CaSO_4$ (0.15%) hydrogel shows the fastest degradability; however, Col–Alg–$CaSO_4$ (0.6%) shows the slowest degradability; depending on the concentration of $CaSO_4$. Moreover, addition of Hap causes slower degradation compared to hydrogels without Hap. However, both composites with Hap, Col-Alg-Hap-$CaSO_4$ (0.3 and 0.6%) exhibit the least degradation ratios, around 25 and 16%, respectively, at day 45. Meanwhile, Col–Alg–$CaSO_4$ (0.15%, 0.30% and 0.6% of $CaSO_4$) shows complete degradation at day 6th, 7th and 8th, respectively. This concludes that the addition of Hap NPs in composite hydrogels causes additional cross-linking, leading to a reduction of the material's elasticity behavior [36].

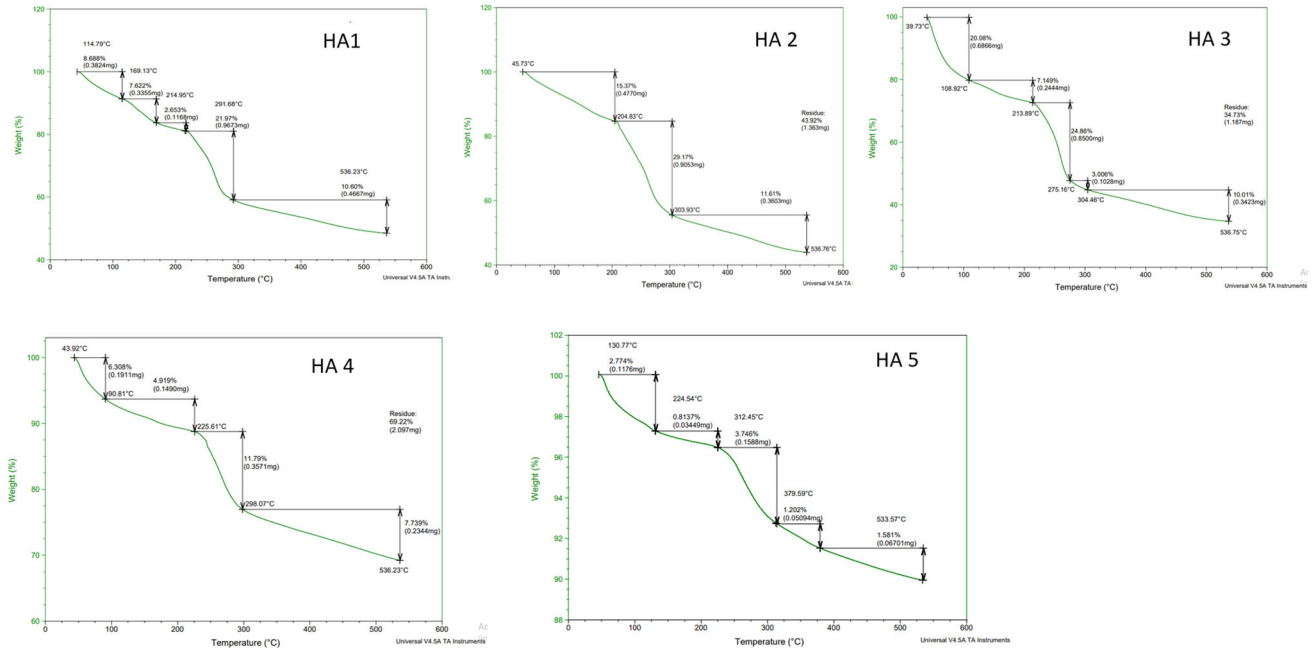

Fig. 8 TGA thermographs of Col–Alg–$CaSO_4$ composite hydrogels

3.6 TGA Results of Col–Alg–$CaSO_4$ Composite Hydrogels

TGA results in Fig. 8 show a slight weight loss in all hydrogels at temperature less than 100 °C, due to the dehydration of moisture, humidity or solvent traces removal in various hydrogels. It also recorded a sharp decrease in mass at 200–300 °C in all hydrogel's formulas. Composite hydrogels coded HA4 and HA5 show ~ 8–25% mass loss, compared to samples coded HA1, HA2 and HA3 which show mass loss ~ 40–50% in the second degradation stage between 200 and 300 °C. This indicates that the addition of Hap NPs into hydrogel provides as a filler action, which causes significant improvement in thermal stability of hydrogels compared to hydrogels Hap free. These observations are consistent with previous results [24]. Notably, HA3 hydrogel exhibits the least thermal stability, due to the inhomogeneity of formed composite hydrogel. There is no significant difference of the mass loss for HA1 and HA2 which indicates that an increase in $CaSO_4$ concentration did not affect the thermal stability, unlike the Hap NPs incorporation which enhanced sharply the thermal stability of accompanied composite hydrogels [38].

3.7 Antimicrobial Activity of Col–Alg–$CaSO_4$ Composite Hydrogels

The bone scaffold-associated infection is a mutual postoperative difficulty, which offers a major challenge in orthopedic surgery [39]. Therefore, assessment of antimicrobial potency of the composite's hydrogel should be assessed carefully. In the current bioassay, the diameters of inhibition zones are generated by the tested formulas (HA1, HA2, HA3, HA4, HA5 and HA6): Collagen (0.01%)/alginate (0.8%) against *Pseudomonas aeruginosa, Escherichia coli, Bacillus cereus, Staphylococcus aureus, Candida albicans* and *Candida krusei*, respectively, were photographed and measured, are shown in Fig. 9 and are summarized in Table 4.

Composite hydrogels codes, such as HA1, HA2, HA3, HA4 and HA5, do not inhibit any of pathogens that are tested. All tested composite hydrogels did not exhibit any detectable antifungal activity against either *Candida albicans* or *Candida krusei* (Table 5). Notably, only HA4 and HA5 composite hydrogels demonstrated limited antibacterial efficacy. However, HA5 hydrogel (Col/Alg/Hap/0.60%$CaSO_4$) has the largest zone of inhibition against *E. coli*, recording 6.54 ± 1.45 mm. When the examined formulations are combined with pathogens in the liquid phase using the broth micro-dilution experiment, no synergistic impact is observed (Fig. 10). However, HA5 hydrogel demonstrates only minimal antimicrobial efficacy against all tested pathogens. As illustrated in Table 5, *E. coli* has the highest growth inhibition rate ($36.86 \pm 4.41\%$), followed by *Pseudomonas aeruginosa* ($28.69 \pm 5.65\%$). This is due to the presence of Hap NPs as previously reported that Hap has limited antibacterial effect. However, the most direct and effective to increase the antibacterial effect is by integrating antibiotic delivery system into hydrogels [39].

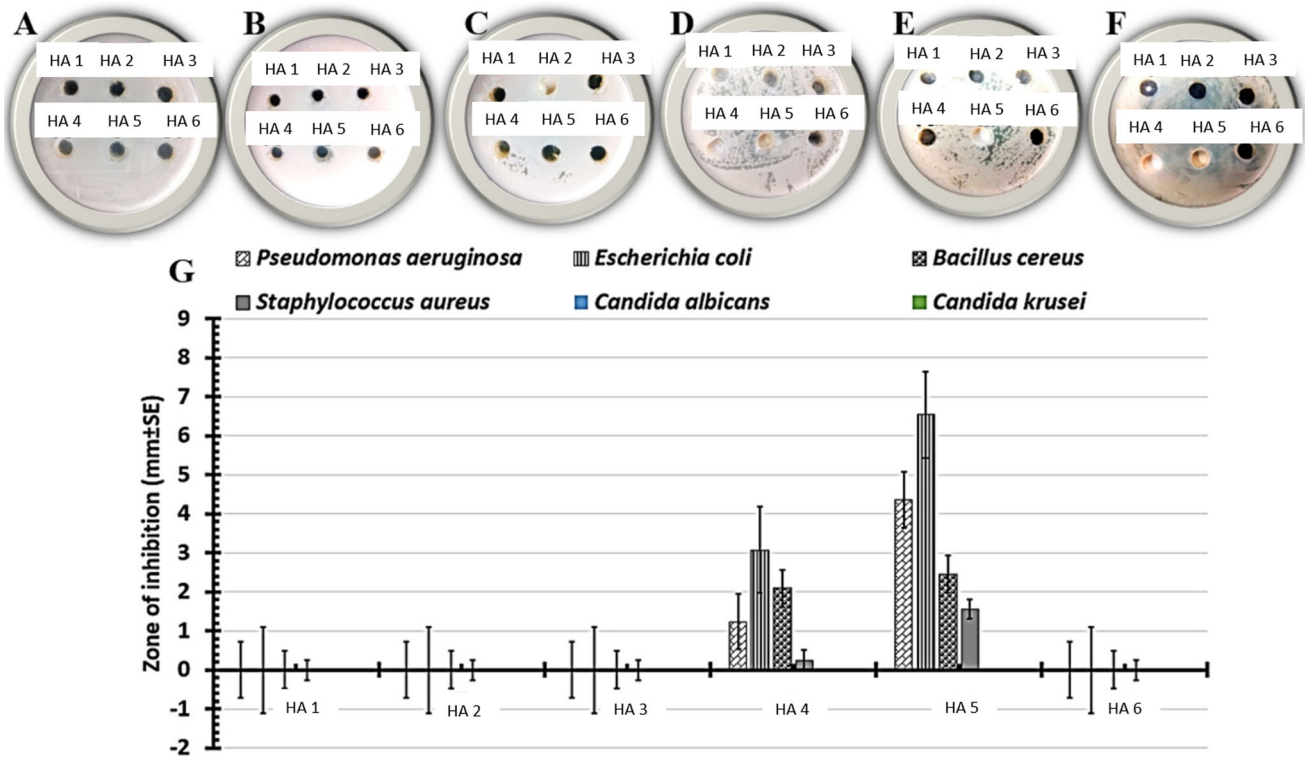

Fig. 9 Inhibition zones formed by composed hydrogels of (HA1): Col (0.01%)/Alg (0.8%)/$CaSO_4$ (0.15%), (HA2): Col (0.01%)/Alg (0.8%)/$CaSO_4$ (0.30%), (HA3): Col (0.01%)/Alg (0.8%)/$CaSO_4$ (0.60%), (HA4): Col (0.01%)/Alg (0.8%)/Hap (1.6%)/$CaSO_4$ (0.30%), (HA5): Col (0.01%)/Alg (0.8%)/Hap (1.6%)/$CaSO_4$ (0.60%) and (HA6): Col (0.01%)/Alg (0.8%) *against* (A) *Pseudomonas aeruginosa*, (B) *Escherichia coli*, (C) *Bacillus cereus*, (D) *Staphylococcus aureus*, (E) *Candida albicans* and (F) *Candida krusei.* The assays were performed in triplicate, and the data are shown as the mean of three data points with standard error (SE)

Table 4 Inhibition zones generated against human pathogens, the tested hydrogels were coded as (HA1): Collagen (0.01%)/alginate (0.08%)/$CaSO_4$ (0.15%), (HA2): Collagen (0.01%)/alginate (0.08%)/$CaSO_4$ (0.30%), (HA3): Collagen (0.01%)/alginate (0.08%)/$CaSO_4$ (0.60%), (HA4): Hap (1.6%)/Collagen (0.01%)/alginate (0.08%)/$CaSO_4$ (0.30%), (HA5): Hap (1.6%)/Collagen (0.01%)/alginate (0.08%)/$CaSO_4$ (0.60%), and (HA6): Collagen (0.01%)/alginate (0.08%) (Significant differences $P < 0.05$)

Multidrug-resistant human pathogens	Inhibition zone (mm ± SD)					
	HA1	HA2	HA3	HA4	HA5*	HA6
Pseudomonas aeruginosa	0 ± 0	0 ± 0	0 ± 0	1.24 ± 0.24	4.36 ± 0.09	0 ± 0
*Escherichia coli**	0 ± 0	0 ± 0	0 ± 0	3.07 ± 0.89	6.54 ± 1.45	0 ± 0
Bacillus cereus	0 ± 0	0 ± 0	0 ± 0	2.09 ± 1.02	2.45 ± 0.01	0 ± 0
Staphylococcus aureus	0 ± 0	0 ± 0	0 ± 0	0.25 ± 0.09	1.56 ± 0.07	0 ± 0
Candida albicans	0 ± 0	0 ± 0	0 ± 0	0 ± 0	0 ± 0	0 ± 0
Candida krusei	0 ± 0	0 ± 0	0 ± 0	0 ± 0	0 ± 0	0 ± 0

3.8 Cytotoxicity Test of Col–Alg–$CaSO_4$ Composite Hydrogels

Results show that all tested composite hydrogels promote the proliferation of *MG-63* cells significantly in a concentration dependent manner, compared to *MG-63* without hydrogels as a positive control after one day of incubation with different concentrations using serial dilutions (200, 100, 50, 25, 12.5 and 6.25 μg/mL), as shown in Fig. 11. Interestingly, HA5 hydrogel contains Hap along with the highest concentration of $CaSO_4$ (0.6%) shows the highest cell viability at all dilutions on *MG-63* cells among all tested hydrogels. Increasing $CaSO_4$ is the main precursor in increasing

Table 5 Turbidity and maximum growth inhibition rate (%SD) achieved against human pathogens

Multidrug-resistant human pathogens	Optical density (at 600 nm ± SD)							Maximum growth inhibition rate (% ± SD)
	Control	HA1	HA2	HA3	HA4	HA5*	HA6	
Pseudomonas aeruginosa	3.45 ± 1.09	3.85 ± 1.24	3.82 ± 1.03	3.19 ± 2.04	2.93 ± 0.32	2.46 ± 0.33	3.25 ± 0.18	28.69 ± 5.65
Escherichia coli *	2.36 ± 0.36	2.34 ± 0.25	2.45 ± 0.65	2.81 ± 0.33	2.54 ± 0.11	1.49 ± 0.03	2.09 ± 1.07	36.86 ± 4.41
Bacillus cereus	2.65 ± 1.04	2.52 ± 1.21	2.35 ± 0.31	2.43 ± 0.51	2.35 ± 0.34	2.09 ± 0.11	2.36 ± 0.21	21.13 ± 2.07
Staphylococcus aureus	3.21 ± 0.97	3.16 ± 0.95	3.25 ± 1.09	3.17 ± 1.12	3.2 ± 1.07	2.63 ± 0.46	2.19 ± 0.08	18.06 ± 8.53
Candida albicans	3.96 ± 1.23	3.56 ± 1.04	4.07 ± 1.32	3.92 ± 1.29	3.82 ± 2.05	3.68 ± 0.7	3.5 ± 2.34	6.89 ± 3.94
Candida krusei	4.23 ± 0.67	4.09 ± 2.17	3.98 ± 1.11	4.12 ± 2.16	4.24 ± 0.34	4.01 ± 0.3	4.19 ± 1.83	5.20 ± 9.45

The tested hydrogels were coded as (HA1): Collagen (0.01%)/alginate (0.08%)/$CaSO_4$ (0.15%), (HA2): Collagen (0.01%)/alginate (0.08%)/$CaSO_4$ (0.30%), (HA3): Collagen (0.01%)/alginate (0.08%)/$CaSO_4$ (0.60%), (HA4): Hap (1.6%)/Collagen (0.01%)/alginate (0.08%)/(0.30%), (HA5): Hap (1.6%)/Collagen (0.01%)/alginate (0.08%)/$CaSO_4$ (0.60%), and (HA6): Collagen (0.01%)/alginate (0.08%) (Significant differences$P < 0.05$)

the cell viability of bone cells. This suggestion is based on previous studies which showed that $CaSO_4$-based scaffolds promote clearly the osteo-conductivity for bone regeneration to promote previously bone healing for critical-sized bone defects [17]. Additionally, *MG-63* cultured with $CaSO_4$ upregulates genetic expressions that are involved in many cellular functions including cell cycle regulation, signaling transduction, immunity and lysosomal enzyme production [40]. Furthermore, it is observed that addition of Hap shows increasing the cell viability of *MG-63* as well. These results are similar to previous reported findings, which showed that Hap NPs have a smaller grain size and higher surface area to allow more cells and proteins to attach on the scaffold surface [34]. In addition, the combination of Hap with scaffolds such as alginate and collagen enhances its brittleness, as well as enhances its osteo-conduction further [34]. Hence, it enhances the ideal properties of a bone subtitle thereby, thus enhancing bone healing and regeneration.

However, cells treated with HA3 with 0.6% $CaSO_4$ with the same concentration are present in HA5, it demonstrates the least cell viability and this result is expected due to the rapid gelation rate of $CaSO_4$ causing unreacted alginate with $CaSO_4$ [3]. However, HA5 with similar concentration of HA3 is observed; unlikely the addition of Hap helps in lowering the gelation rate allowing $CaSO_4$ to be dispersed more evenly throughout the solution for a longer time, this allowed homogenous hydrogel distribution and hence more bounded $CaSO_4$ with alginate.

3.9 Cell Adhesion Test of Col–Alg–$CaSO_4$ Composite Hydrogels

Basically, cell adhesion is a complex route that is intricate in migration, tissue remodeling and wound healing. These processes occur when cells attach to extracellular matrix components through adhesion receptors, in order to bind to the cytoskeleton. Cell motility, proliferation and differentiation and survival are untimely affected by cell adhesion. Results revealed that all tested composite hydrogels coded HA1, HA2, HA3, HA4 and HA5 clearly allow the adhesion of *MG-63* cells, as shown in Fig. 12. Also, all tested composite hydrogels clearly enhance the initial adhesion of cells onto the hydrogel surface. Based on the current and previous results, collagen is a key player for cell adhesion. Collagen I is a major component of extracellular matrices, which has *Arg-Gly-Asp* (RGD) groups that responsible for the interaction between cell and microenvironment [41, 42]. Meanwhile, $CaSO_4$ is *osteo*-conductive materials act as a main material which permits bone cells (*osteoblasts* and *osteoclasts*) to fasten, migrate, grow and/or differentiate [43]. Furthermore, Hap is also considered as a component that promotes cell adhesion. Based on

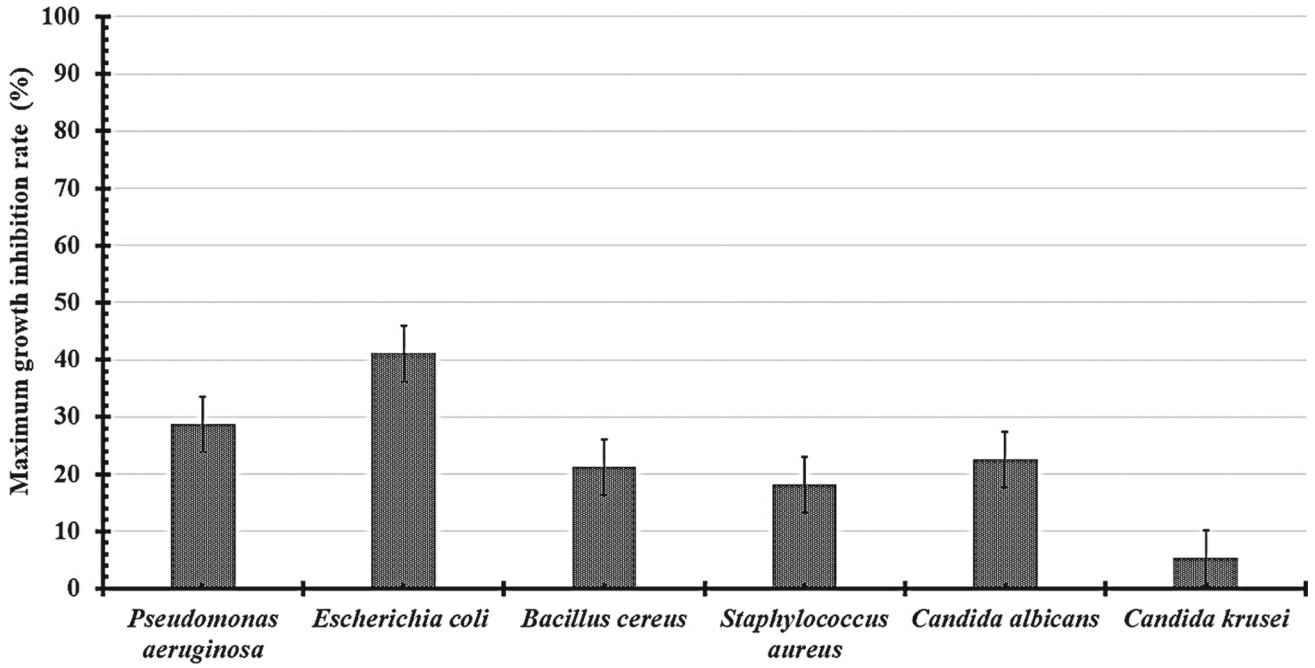

Fig. 10 Histograms of the maximum growth inhibition rates against human pathogens that are achieved using HA5 formula that contained; (0.01% Col, 0.8% Alg, 1.6% Hap and 0.60% $CaSO_4$)

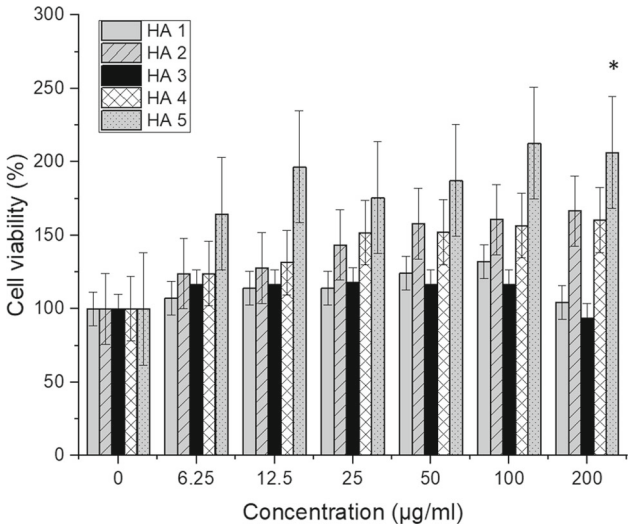

Fig. 11 Cell viability (%) of Col–Alg–$CaSO_4$ composite hydrogels, on osteoblast-like cells (*MG-63* cell line) after one day of incubation. Data are presented as mean ± SD and are subjected to one-way *ANOVA* followed by post hoc (LSD) test at $P < 0.05$. * is significantly different and is marked by the star symbol for major differences compared to other hydrogels

previous results, addition of Hap causes increase in the expression levels of eEF1Bα, γ-actin and adhesion-related proteins through stimulating cell attachment in case of Hap-coated silicone rubber, in comparison with non-coated one [44].

4 Conclusions

- A novel injectable composite hydrogel containing the necessary components to promote bone tissue regeneration and suitable for clinical handling in surgical settings, was successfully prepared and optimized.
- Collagen, alginate and $CaSO_4$ with/without Hap NPs incorporation can form a successful injectable hydrogel without inducing toxic cross-linkers or external factors such as high temperature/change in pH and have rapid gelation rate. As observed from the presented results, addition of high concentration of $CaSO_4$ in the composite hydrogel showed direct proportion in the gelation rate, low swelling index and high cell viability of osteoblast-like cells (*MG-63*); and has an inverse effect on the degradation rate of formed composite hydrogel.
- Incorporation of Hap lowered and significantly controlled the gelation rate and allowed formation of more uniform hydrogel. Hydrogels with Hap showed significant swelling index, enhancement in the thermal stability, as well as improvement in the cell viability and antimicrobial activity of the composite hydrogel.
- Injectable hydrogels can apply for a wide range of bone regeneration applications; particularly filling the irregular defects such as the cavitary bone defects and enhancing bone growth in this area. Such results support the use of the synthesized injectable hydrogel in the future as a carrier for mesenchymal stem cells/growth factors to further improve bone formation.

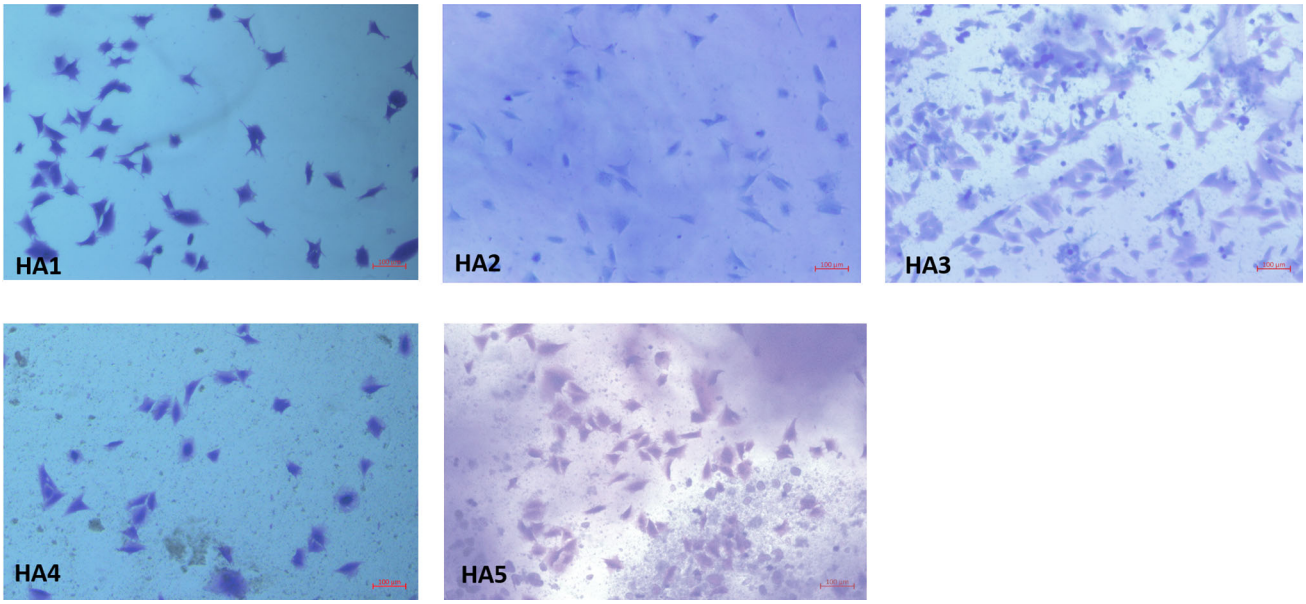

Fig. 12 Inverted microscope images of *MG-63* cell line adhered on Col–Alg–$CaSO_4$ composite hydrogel without and with hydroxyapatite using crystal violet staining, (image scale 100μm, and original magnification X200)

Supplementary Information The online version contains supplementary material available at https://doi.org/10.1007/s13369-024-08922-w.

Acknowledgements Authors thank Dr. Med. Ahmed Ghomeimy, Regenerative Medicine Laboratory, Department of Basic Research, Children's Cancer Hospital 57357, Cairo, Egypt, for donation of collagen. This work was supported by the Deanship of Scientific Research, Vice Presidency for Graduate Studies and Scientific Research, King Faisal University, Saudi Arabia [GRANT 5981].

Author's Contribution HA was involved in experimental work and wrote the original manuscript; SS wrote the original and revised the manuscript; SE-M conducted the microbiology part; SL conducted the cell culture experiments, and EK helped in supervision, wrote the original and revised the manuscript.

Funding No funding was received for conducting this work.

Data Availability All data are available.

Declarations

Conflict of interest The authors declare no competing of interests.

Consent for Publication Available publications for all data and figures.

Ethical Approval No animal model, human trials or *In-vivo* experiments were carried out in this research. All research studies followed the Helsinki World Medical Association's Declaration: Ethical Medical Research Principles Involving Human Subjects.

References

1. Arif, Z.U., et al.: Recent advances in 3D-printed polylactide and polycaprolactone-based biomaterials for tissue engineering applications. Int. J. Biol. Macromol. (2022). https://doi.org/10.1016/j.ijbiomac.2022.07.140
2. Arif, Z.U., et al.: Biopolymeric sustainable materials and their emerging applications. J. Environ. Chem. Eng. **10**(4), 108159 (2022)
3. Bendtsen, S.T.; Wei, M.: Synthesis and characterization of a novel injectable alginate-collagen-hydroxyapatite hydrogel for bone tissue regeneration. J Mater Chem B **3**(15), 3081–3090 (2015)
4. Zhang, Y., et al.: Hydrogel: a potential therapeutic material for bone tissue engineering. AIP Adv. **11**, 010701 (2021)
5. Arif, Z.U., et al.: Additive manufacturing of sustainable biomaterials for biomedical applications. Asian J. Pharm. Sci. (2023). https://doi.org/10.1016/j.ajps.2023.100812
6. Hu, W., et al.: Advances in crosslinking strategies of biomedical hydrogels. Biomater. Sci. **7**(3), 843–855 (2019)
7. Dodda, J.M.; Azar, M.G.; Sadiku, R.: Crosslinking trends in multicomponent hydrogels for biomedical applications. Macromol. Biosci. **21**(12), e2100232 (2021)
8. Duquette, D.; Dumont, M.-J.: Comparative studies of chemical crosslinking reactions and applications of bio-based hydrogels. Polym. Bull. **76**(5), 2683–2710 (2018)
9. Arif, Z.U., et al.: 4D bioprinting of smart polymers for biomedical applications: recent progress, challenges, and future perspectives. React. Funct. Polym. (2022). https://doi.org/10.1016/j.reactfunctpolym.2022.105374
10. Noroozi, R., et al.: 3D and 4D bioprinting technologies: A game changer for the biomedical sector? (1573–9686 (Electronic))
11. Arif, Z.U., et al.: A review on four-dimensional (4D) bioprinting in pursuit of advanced tissue engineering applications. Bioprinting **27**, e00203 (2022)
12. Hernández-González, A.C.; Téllez-Jurado, L.; Rodríguez-Lorenzo, L.M.: Alginate hydrogels for bone tissue engineering, from injectables to bioprinting: a review. Carbohydr. Polym. **229**, 115514 (2020)

13. Grant, G.T., et al.: Biological interactions between polysaccharides and divalent cations: the egg-box model. FEBS Lett. **32**(1), 195–198 (1973)
14. Bidarra, S.J.; Barrias, C.C.; Granja, P.L.: Injectable alginate hydrogels for cell delivery in tissue engineering. Acta Biomater. **10**(4), 1646–1662 (2014)
15. Yao, R., et al.: Alginate and alginate/gelatin microspheres for human adipose-derived stem cell encapsulation and differentiation. Biofabrication (2012). https://doi.org/10.1088/1758-5082/4/2/025007
16. Hu, T.; Lo, A.C.Y.: Collagen-alginate composite hydrogel: application in tissue engineering and biomedical sciences. Polymers (Basel) (2021). https://doi.org/10.3390/polym13111852
17. Huang, K.H., et al.: Incorporation of calcium sulfate Dihydrate into a mesoporous calcium silicate/poly-Epsilon-Caprolactone scaffold to regulate the release of bone morphogenetic Protein-2 and accelerate bone regeneration. Biomedicines (2021). https://doi.org/10.3390/biomedicines9020128
18. Sargeant, T.D., et al.: An in situ forming collagen-PEG hydrogel for tissue regeneration. Acta Biomater. **8**(1), 124–132 (2012)
19. Arif, Z.U., et al.: 3D printing of stimuli-responsive hydrogel materials: literature review and emerging applications. Giant (2023). https://doi.org/10.1016/j.giant.2023.100209
20. Fernandes, G.; Abhyankar, V.; O'Dell, J.M.: Calcium sulfate as a scaffold for bone tissue engineering: a descriptive review. Journal of Dentistry, Oral Disorders & Therapy **9**(1), 1–22 (2021)
21. Alfotawi, R., et al.: Assessment of cellular viability on calcium sulphate/hydroxyapatite injectable scaffolds. J. Tissue Eng. **4**, 2041731413509645 (2013)
22. Kim, J.H., et al.: Grafting using injectable calcium sulfate in bone tumor surgery: comparison with demineralized bone matrix-based grafting. Clin. Orthop. Surg. **3**(3), 191–201 (2011)
23. Yan, T.T., et al.: Porous calcium sulfate/hydroxyapatite whiskers scaffold for bone tissue engineering. Adv. Mater. Res. **738**, 38–41 (2013)
24. Salim, S.A., et al.: Influence of chitosan and hydroxyapatite incorporation on properties of electrospun PVA/HA nanofibrous mats for bone tissue regeneration: nanofibers optimization and in-vitro assessment. J. Drug Deliv. Sci. Technol. (2021). https://doi.org/10.1016/j.jddst.2021.102417
25. Giannoudis, P.V.; Dinopoulos, H.; Tsiridis, E.: Bone substitutes: an update. Injury **36**(Suppl 3), S20–S27 (2005)
26. Russo, L., et al.: Carbonate hydroxyapatite functionalization: a comparative study towards (bio)molecules fixation. Interface Focus **4**(1), 20130040 (2014)
27. Wang, H., et al.: Biocompatibility and osteogenesis of biomimetic nano-hydroxyapatite/polyamide composite scaffolds for bone tissue engineering. Biomaterials **28**(22), 3338–3348 (2007)
28. Wiegand, I.; Hilpert, K.; Hancock, R.E.: Agar and broth dilution methods to determine the minimal inhibitory concentration (MIC) of antimicrobial substances. Nat. Protoc. **3**(2), 163–175 (2008)
29. Hayat, S., et al.: Biofabrication of ZnO nanoparticles using Acacia arabica leaf extract and their antibiofilm and antioxidant potential against foodborne pathogens. PLoS ONE **17**(1), e0259190 (2022)
30. Thi-Hiep, N.; Hoa, D.V.; Toi, V.V.: Injectable in situ crosslinkable hyaluronan-polyvinyl phosphonic acid hydrogels for bone engineering. J. Biomed. Sci. Eng. **06**(08), 854–862 (2013)
31. Wu, P., et al.: Biological effects different diameters of Tussah silk fibroin nanofibers on olfactory ensheathing cells. Exp. Ther. Med. **17**(1), 123–130 (2019)
32. El-Fiqi, A.; Kim, J.H.; Kim, H.W.: Novel bone-mimetic nanohydroxyapatite/collagen porous scaffolds biomimetically mineralized from surface silanized mesoporous nanobioglass/collagen hybrid scaffold: Physicochemical, mechanical and in vivo evaluations. Mater. Sci. Eng. C Mater. Biol. Appl. **110**, 110660 (2020)
33. Serhiienko, A., et al.: Synthesis and characterization of hydroxyapatite and composite based on it with collagen/alginate. Chem. Pap. **76**(1), 385–392 (2021)
34. Bal, Z., et al.: Bone regeneration with hydroxyapatite-based biomaterials. Emergent. Mater. **3**(4), 521–544 (2019)
35. Yang, L., et al.: High-throughput methods in the discovery and study of biomaterials and materiobiology. Chem. Rev. **121**(8), 4561–4677 (2021)
36. Jana, S., et al.: High-strength pristine porous chitosan scaffolds for tissue engineering. J. Mater. Chem. (2012). https://doi.org/10.1039/C2JM16676C
37. Kostenko, A.; Swioklo, S.; Connon, C.J.: Effect of Calcium sulphate pre-crosslinking on rheological parameters of alginate based bio-inks and on human corneal stromal fibroblast survival in 3D bio-printed constructs. Front. Mech. Eng. (2022). https://doi.org/10.3389/fmech.2022.867685
38. Shuai, C., et al.: Enhanced stability of calcium sulfate scaffolds with 45S5 bioglass for bone repair. Materials (Basel) **8**(11), 7498–7510 (2015)
39. Ji, X.-J., et al.: Corrosion resistance and antibacterial effects of hydroxyapatite coating induced by polyacrylic acid and gentamicin sulfate on magnesium alloy. Front. Mater. Sci. **13**(1), 87–98 (2019)
40. Carinci, F., et al.: Calcium sulfate: analysis of MG63 osteoblast-like cell response by means of a microarray technology. J. Biomed. Mater. Res. B Appl. Biomater. **71**(2), 260–267 (2004)
41. Jin, G.Z.; Kim, H.W.: Efficacy of collagen and alginate hydrogels for the prevention of rat chondrocyte dedifferentiation. J Tissue Eng **9**, 2041731418802438 (2018)
42. Rajan, N., et al.: Preparation of ready-to-use, storable and reconstituted type I collagen from rat tail tendon for tissue engineering applications. Nat. Protoc. **1**(6), 2753–2758 (2006)
43. Sirka, A., et al.: Calcium sulphate/hydroxyapatite carrier for bone formation in the femoral neck of osteoporotic rats. Tissue Eng. Part A **24**(23–24), 1753–1764 (2018)
44. Shi, X.H., et al.: Hydroxyapatite-coated sillicone rubber enhanced cell adhesion and it may be through the interaction of EF1beta and gamma-actin. PLoS ONE **9**(11), e111503 (2014)